Electron Holography with Atomic Focusers

J. M. Cowley
Department of Physics and Astronomy, Arizona State University, Tempe, Arizona 85287-1504
(Received 16 November 1999)

In a modified form of electron holography, as originally proposed by Gabor, a specimen illuminated by the focused, convergent beam of a scanning transmission electron microscope is followed by a thin crystal which acts as a periodic array of atomic focusers. Each of the broad diffraction spots of the crystal then contains a magnified image of the specimen with a resolution limit of 0.05 nm or less. The method is illustrated by images of crystal lattice planes and tungsten atoms in the diffraction patterns formed by crystals in the walls of carbon nanoshells.

PACS numbers: 61.14.Nm, 61.14.Lj, 61.48.+c

In recent years, many papers purporting to deal with the subject of "electron holography" (or "x-ray holography") initially quote Gabor [1] as the originator of the holography concept, but then describe theory or experiment on the derivation from diffraction data of real-space information on relative atomic positions, averaged over large assemblies of atoms. Gabor's ideas on holography referred to imaging in the accepted sense of a one-to-one correspondence of image features (black or white dots) with individual atom positions. Electron holography according to the scheme originally proposed by Gabor has been shown to be feasible [2], and many variations on the technique of electron holography have been shown to be possible and of practical value [3–6] (despite misleading statements made in apparent ignorance of this literature [7]). Similarly, x-ray holography in the true Gabor sense has been widely investigated, and various workers have achieved important progress in this respect [8,9].

The so-called electron holography based on the analysis of the intensities of diffraction patterns for electrons generated from, or scattered by, atoms within the sample, has had important successes, particularly for the analysis of thin surface layers [10]. However, these diffraction pattern analyses do not constitute electron holography in the Gabor sense. They follow on from the tradition of interpretation of diffraction effects facilitated by the use of scattering from reference atoms, as initiated by Bragg [11] and developed by many others in subsequent years (heavy atom methods, anomalous scattering methods, etc., as described in any textbook on x-ray crystallography). It has been suggested that the term "holographic diffraction" may be appropriate for these methods [12].

In the modern version of Gabor's original scheme [1,2], a small crossover is formed by electromagnetic lenses, as in a scanning transmission electron microscopy (STEM) instrument, close to a thin specimen. The greatly magnified "point-projection" image produced at a large distance beyond the specimen is recorded as the hologram, and is processed by optical or digital methods to correct for the aberrations of the probe-forming lens, thus giving improved resolution. The directly transmitted, "unscattered" radiation serves as a reference wave providing phase information by interference with the radiation scattered by the object.

Alternative versions of this scheme, offering means for resolution enhancement not involving the often difficult step of correcting for the lens aberrations, are now possible through the availability of much smaller electron sources. For low energy electrons (in the range of 50–200 eV) very small, single-atom, field-emission points can be used [13]. For higher energy electrons (energies in the electron microscope range of 100–400 keV), atomic focusers may provide such sources [14–18].

The initial theoretical treatment by Smirnov [14] showed that single heavy atoms, or rows of atoms extending through a thin crystal, have a focusing effect on an incident electron wave and can give focused crossovers of diameter 0.05 nm or less. Used as the final beam-forming lens in a STEM instrument, an atomic focuser could thus give a resolution of 0.05 nm or better, as compared with the resolution limit of normal STEM instruments of about 0.2 nm. It was subsequently shown by Cowley *et al.* [15] that equivalent imaging configurations using the plane-wave illumination of a normal transmission electron microscopy (TEM) instrument could give the same resolution enhancement. Also thin crystals could act as periodic arrays of atomic focusers so that other schemes, involving the self-imaging effects of coherent periodic arrays of emitters or scatterers (the formation of Fourier images) could be envisaged.

One such scheme is illustrated in Fig. 1. A thin object is illuminated by the focused beam from a STEM instrument and is followed at a distance R by a thin crystal in axial orientation. It has been shown that, for such crystals of relatively simple structure, channeling of the electrons along the rows of atoms parallel to the incident beam direction can have the effect of producing a periodic array of crossovers at the exit face, each sharp intensity maximum having a diameter of 0.05 nm or less [15–18].

The portion of the focused, convergent beam that is transmitted without scattering by the object forms a convergent-beam electron diffraction pattern of the crystal at infinity, with each diffraction spot enlarged to form a disk. This diffraction pattern acts as a reference wave

 0031-9007/00/84(16)/3618(4)$15.00

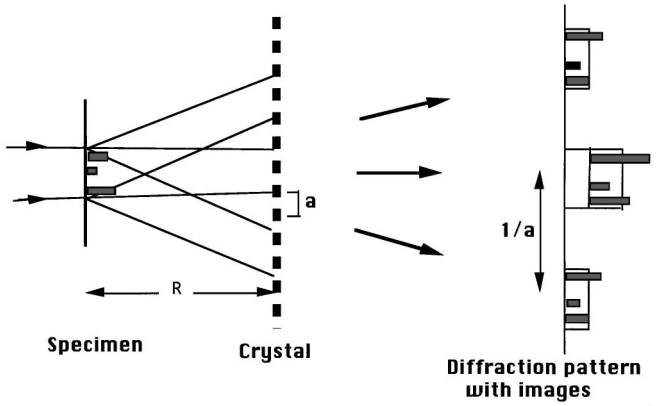

FIG. 1. Diagram suggesting the holographic imaging method. The convergent beam in a STEM instrument is focused on a thin specimen held at a Fourier image distance R from a thin crystal. Magnified images of the specimen appear within the diffraction spots of the crystal.

for the hologram. The waves scattered by the object are rescattered by the crystal and generate a Fourier image at infinity if the distance of the object from the crystal is a Fourier-image distance, $R = 2na^2/\lambda$ (for the one-dimensional case), where a is the periodicity of the crystal, λ is the electron wavelength, and n is an integer. It may be considered that each point of the object acts as a source to form a Fourier image of the crystal, as a periodic array of points (or of directions for the Fourier image at infinity), each spread by the dimensions of the individual crossovers formed by the rows of atoms of the crystal. Addition of the Fourier images from all points of the object then gives rise to a periodic array of images of the illuminated region of the object with a resolution equal to the diameter of the crossovers, namely, 0.05 nm or less. Interference of this array of images with the reference wave, the convergent-beam diffraction pattern of the crystal, then gives a modulation of the diffraction spots so that each spot shows a magnified, high-resolution image of the specimen. The zero spot of the diffraction pattern contains the same image but with a large background term due to the directly transmitted beam [19]. A detailed theoretical treatment of this process is given elsewhere [19,20].

The practical difficulties involved in the realization of this scheme include the problem of holding a small thin object at the Fourier-image distance, of the order of 10–100 nm, from a suitable thin crystal. A convenient solution to this problem has been found in the use of carbon nanoshells. These are hollow, near-spherical shells of graphitic carbon [21] which may sometimes be approximately 100 nm in diameter with walls 10–30 nm thick. The walls are composed of thin graphite crystal layers 5–10 nm thick and mutually rotated about their common c axes [22]. The graphite crystal layers are not ideal for the purpose, being imperfect, overlapping crystals of undefined thickness and orientation, but serve the purpose of providing a convenient test for the imaging method.

When the convergent beam in a STEM instrument is focused on the middle of such a nanoshell, one of the graphite crystals in one wall of the nanoshell may act as an atomic-focuser crystal to produce images of some part of the opposite wall of the nanoshell. Then the large diffraction spots from the focuser crystal contain fringe patterns corresponding to the lattice plane spacings of the graphite in the imaged specimen area. Figure 2, for example, shows diffraction patterns obtained with a 100 keV STEM instrument in which the diffraction spots contain fringes differing in spacing by a factor of $3^{1/2}$. Since diffraction patterns from these areas show only the reflections from the (100) and (110) graphite planes with any appreciable intensity, the fringes must correspond to the periodicities of 0.215 and 0.125 nm for these planes, respectively [19]. This suggests a resolution improvement since the STEM instrument as used (with $C_s = 1.0$ mm and an aperture angle of 1.1×10^{-2} rad) has a resolution for normal STEM imaging of no better than about 0.35 nm, usually degraded to about 0.5 nm or more by mechanical vibrations of the specimen stage.

Since the imaging of periodic objects represents a special case, resolution tests are preferably carried out on nonperiodic objects of known structure. It was shown by Iijima [23] that if tungsten is evaporated on graphite it tends to eat away the atom-thick surface layers of the graphite, forming extended atomically smooth surfaces with occasional atom-high steps. Single atoms or small clumps of atoms of tungsten appear to be attached to the steps. We

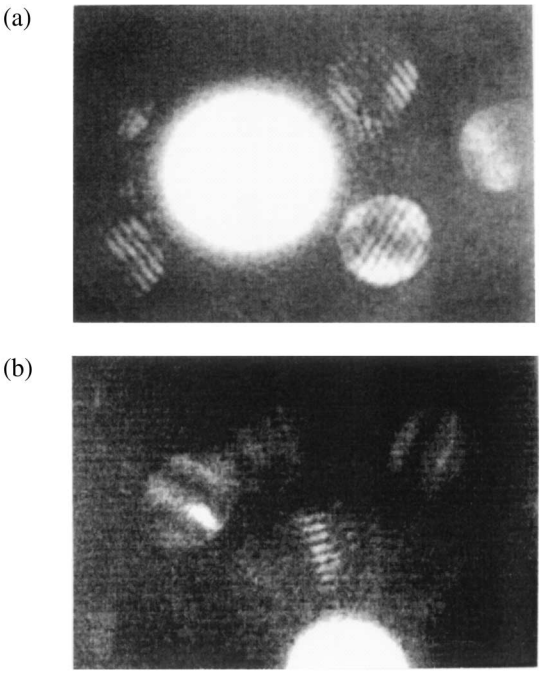

FIG. 2. Fringe images formed within diffraction spots as a crystal within one wall of a carbon nanoshell acts as an atomic focuser to give images of parts of the opposite wall. The fringe spacings correspond to the 0.215 and 0.125 nm spacings of the (100) and (110) graphite planes. (a) Shows two-dimensional fringes. (b) Shows finer fringes in the outer spots.

therefore have evaporated tungsten on the carbon nanoshells in an attempt to obtain a distribution of single tungsten atoms as a suitable test specimen for the atomic-focuser imaging. Simulations of the transmission of 100 keV electrons through graphite crystals have suggested that the atomic-focuser imaging in this configuration should give resolutions of about 0.06 nm [20].

The partial diffraction patterns of Fig. 3 were recorded with a charge-coupled device (CCD) detector. The central spot of the diffraction pattern was deflected to one side so that the full range of intensities recorded by the CCD could be used for the other diffraction spots. The broad spots form two diffuse rings corresponding to the (100) and (110) graphite spacings. Fringes within the diffraction spots provide a calibration of the image magnification. There is usually a diffuse background to the images arising from scattering by the specimen and by the crystals for which the Fourier imaging condition is not satisfied.

The individual diffraction disks contain some single black and white spots which could possibly correspond to individual heavy atoms. Without the evaporated tungsten, no such spots appeared. With the tungsten, some dark spots appeared in high-resolution TEM images of the nanoshells. The theoretical treatment [19,20] suggests that, as in normal high-resolution TEM or STEM imaging, the images of atoms in the diffraction disks should be dark for underfocus and white for overfocus and of variable size, depending on the defocus. Since, for this case, the spots may be given by several superimposed graphite crystals, the imaging may be underfocused for some diffraction spots and overfocused for others. The spot diameters vary but, by comparison with the 0.125 nm fringe spacings of the outer ring of Fig. 3(a), for example, the diameters may be as small as about 0.06 nm.

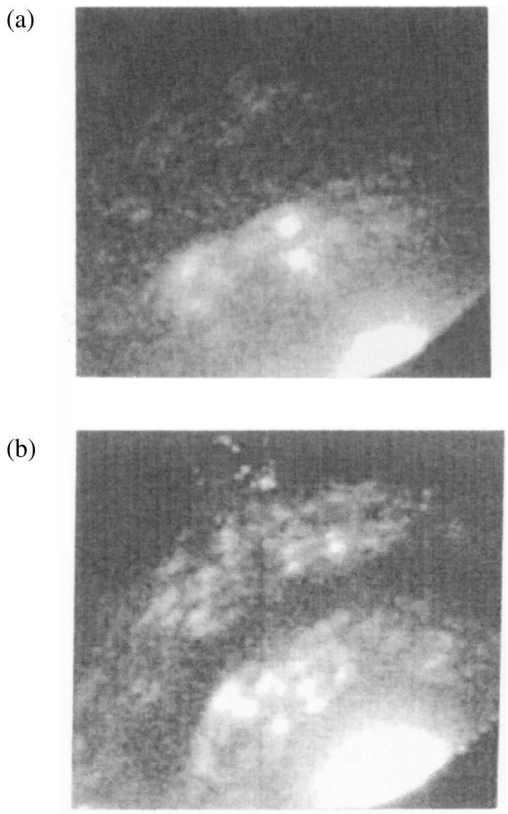

FIG. 3. Partial diffraction patterns with the central spot displaced to one side of the CCD detector. Within the diffraction spots there are small white and [especially in (b)] black spots, considered to be images of tungsten atoms evaporated on one wall of a carbon nanoshell and imaged by the atomic-focuser effect of a graphite crystal within the other wall of the nanoshell.

The theoretical treatment [20] shows that, for the simplest (one-dimensional) case of a weak phase object having a projected potential distribution $\varphi(x)$, and an atomic focuser crystal for which each sharp amplitude peak at the exit face has a distribution $f_0(x)$, the h diffraction spot has an intensity distribution, close to the optimum, "Scherzer," defocus, given by

$$I_h(u) = F_h^2 A(u)[1 + f_0(R\lambda u) * 2\sigma\varphi(R\lambda u)s(R\lambda u)],$$

where F_h is the structure amplitude for the h reflection, u is the angular variable equal to $(2/\lambda)\sin(\phi/2)$, where ϕ is the scattering angle, $A(u)$ is the aperture function for the probe-forming lens, σ is the interaction constant, and $s(x)$ is the spread function given by Fourier transform of the imaginary part of the transfer function of the lens. The $*$ symbol represents a convolution operation.

It is thus seen that the resolution is given by the width of the $f_0(x)$ function and the magnification of the image is inversely proportional to the separation R. The imaged area is limited by the aperture function, $A(u)$, or by the width of the spread function, $s(x)$. Both widths are normally made to be about 1 nm. Images for larger areas may possibly be accumulated by recording many images with shifts of the incident beam or of the specimen.

It thus appears likely that this holographic imaging process making use of the atomic-focuser effects is capable of producing images having resolutions close to 0.06 nm in this case and, if used with suitable thin single crystals of gold or other heavy element, should give resolutions approaching 0.03 nm. Remaining difficulties for the wider application of the method include the limitations of the image areas and the problems of preparing suitable combinations of thin specimens and thin, suitably oriented, crystals held rigidly with respect to each other with separations of 10–100 nm.

We thank undergraduate student Jacob Hudis for assistance, particularly with the computer simulations, Dr. David Smith for associated high-resolution electron microscopy and for useful comments, and John Wheatley and Alan Higgs of the ASU Center for High Resolution Electron Microscopy for valuable technical support.

[1] D. Gabor, Nature (London) **161**, 777 (1948); Proc. R. Soc. London A **197**, 454 (1949).

[2] J. A. Lin and J. M. Cowley, Ultramicroscopy **19**, 179 (1986).

[3] J. M. Cowley, Ultramicroscopy **41**, 335 (1992).
[4] *Electron Holography,* edited by A. Tonomura *et al.* (Elsevier, Amsterdam, 1995).
[5] *Introduction to Electron Holography,* edited by E. Völkl, L. F. Allard, and D. C. Joy (Kluwer Academic/Plenum Publishing, New York, 1998).
[6] D. Van Dyck, H. Lichte, and K. D. van der Mast, Ultramicroscopy **64**, 1 (1996).
[7] S. G. Bompadre, T. W. Peterson, and L. B. Sorensen, Phys. Rev. Lett. **83**, 2741 (1999).
[8] J. McNulty, Nucl. Instrum. Methods Phys. Res., Sect. A **347**, 170 (1994).
[9] J. Kirz, C. Jacobsen, and M. Howells, Q. Rev. Biophys. **28**, 1 (1995).
[10] D. K. Saldin, Surf. Rev. Lett. **4**, 441 (1997), and the following papers.
[11] W. L. Bragg, Z. Kristallogr. **70**, 483 (1929).
[12] J. M. Cowley, Surf. Sci. **298**, 336 (1993).
[13] H. W. Fink, H. Schmid, H. J. Kreuzer, and A. Wierzbicki, Phys. Rev. Lett. **67**, 1543 (1991).
[14] V. V. Smirnov, J. Phys. D **31**, 1548 (1998).
[15] J. M. Cowley, J. C. H. Spence, and V. V. Smirnov, Ultramicroscopy **68**, 135 (1997).
[16] J. M. Cowley, R. E. Dunin-Borkowski, and M. Hayward, Ultramicroscopy **72**, 223 (1998).
[17] M. Sanchez and J. M. Cowley, Ultramicroscopy **72**, 213 (1998).
[18] R. E. Dunin-Borkowski and J. M. Cowley, Acta Crystallogr. Sect. A **55**, 119 (1999).
[19] J. M. Cowley, Ultramicroscopy **81**, 47 (2000).
[20] J. M. Cowley and J. B. Hudis, Microsc. Microanal. (to be published).
[21] S. Seraphin, D. Zhou, and J. Jiao, Acta Microsc. **3**, 45 (1994).
[22] J. M. Cowley and C.-H. Kiang, Carbon (to be published).
[23] S. Iijima, Micron **8**, 41 (1977).